A NEW DISTRIBUTED TARGET EXTRACTION METHOD FOR POLARIMETRIC SAR CALIBRATION

Bowen Chi[1*], Jixian Zhang[2], Lijun Lu[3], Shucheng Yang[3], Guoman Huang[3]

[1]Jiangsu Key Laboratory of Resources and Environmental Information Engineering, China University of Mining and Technology, Xuzhou 221116, China - cumtcbw@126.com
[2]Department of Land Surveying and Mapping, Ministry of Natural Resources, Beijing 100812, China - zhangjix@casm.ac.cn
[3]Chinese Academy of Surveying & Mapping, Beijing 100830, China - (lulj, yangsc@casm.ac.cn), huang.guoman@163.com

KEY WORDS: SAR, PolSAR, polarimetric calibration, distributed targets, hypothesis testing, data preprocessing.

ABSTRACT:

Polarimetric calibration is one of the preprocessing steps in the quantitative processing of Polarimetric synthetic aperture radar (PolSAR) data, and its accuracy will affect subsequent applications. At present, the polarimetric calibration method based on distributed targets is widely used, and this kind of method needs to extract distributed targets that satisfy certain scattering characteristics as the calibration reference ground object samples before calibrating. Therefore, the extraction accuracy of distributed targets has a great influence on the accuracy of polarimetric calibration methods based on such targets. Therefore, this paper proposes a new distribution target extraction method, which is based on the idea of KS hypothesis testing, and uses the homogeneity of the pixels in the window to determine whether it is a distribution target. To verify the effectiveness of the method, the X-band airborne PolSAR images are used as the data of the polarimetric calibration experiment. Experiments show that, compared with other extraction methods, our method can not only ensure the extraction accuracy of distributed targets, but also further improve the accuracy of polarimetric calibration.

1. INTRODUCTION

Polarimetric synthetic aperture radar (PolSAR) records the backscattering characteristics of ground objects by transmitting and receiving electromagnetic waves of different polarization states. PolSAR uses the acquired multi-channel amplitude and phase information to extract target parameters, which greatly enhances the ability of earth observation (Lee and Pottier, 2009). Based on this, the application range and scenarios of PolSAR have expanded rapidly, and it has been widely used in many fields such as disaster monitoring (Niu et al., 2021; Park and Lee, 2019), land object classification (Imani, 2021), and vegetation biomass inversion (Mandal et al., 2019; Sajjad et al., 2019).

In 1950, Sinclair(Sinclair, 1950) proposed the use of a second-order complex matrix to describe the polarization scattering characteristics of the target intuitively and comprehensively. However, due to the errors caused by the transceiver antenna, the propagation environment and noise, measurements via the Sinclair matrix were distorted to a certain extent. Polarimetric calibration is an indispensable preprocessing step in the quantitative processing of PolSAR data, and its calibration accuracy will directly affect the effects of many subsequent applications (Zebker et al., 1987). For example, it leads to the deviation of disaster monitoring results, which affects the judgment of disaster severity, etc. Polarimetric calibration restores the distorted measurement Sinclair matrix as much as possible by solving the error model and parameters, thereby obtaining the real scattering matrix information of the target, and ensuring the accuracy and repeatability of PolSAR measurement data in application (Freeman, 1992; Jäger et al., 2019). Usually, the polarimetric calibration can be further divided into two types: point target calibration method (Touzi et al., 2013; Whitt et al., 1991) and distributed target calibration method (Ainsworth et al., 2006; Klein, 1992; Quegan, 1994; Van Zyl, 1990) according to the type of calibration body.

Point target calibration methods, such as the Whitt method (Whitt et al., 1991), rely entirely on corner reflectors (CRs), using artificially deployed active and passive CRs as the basis for calibration. The point target calibration method is accurate and objective, but its accuracy is limited by the distance between the point targets, so in practical applications, it should be selected under the premise of judging its applicability.
Distributed target calibration methods, such as the Quegan method (Quegan, 1994), use some natural distributed features with known scattering characteristics to provide calibration references for crosstalk and cross-pol channel imbalance calibration, and then use other known CRs to correct the imbalance of the co-pol channel. These algorithms usually provide stable antenna reciprocity, target scattering reciprocity and other polarization feature constraints for polarimetric calibration based on some typical distributed natural features such as forests, deserts, bare soil, and farmland. Therefore, to obtain a better polarimetric calibration effect, it is necessary to accurately extract the ground objects that meet the conditions from the image as the polarimetric calibration reference samples before calibrating.

The current reference ground feature extraction methods widely used in polarimetric calibration usually only use polarization features such as total scattering power Span or polarization correlation coefficient (PCC) for extraction (Ainsworth et al., 2006; Kimura et al., 2004), and the results are less accurate. In addition, most of them only use empirical thresholds for extraction, resulting in a limited scope of application of the algorithm. Therefore, if based on the inaccurate extraction results, it is inappropriate to use the calibration method proposed for the scattering characteristics of the distributed target, which will further lead to the unreliability of the

* Corresponding author

https://doi.org/10.5194/isprs-annals-X-3-W1-2022-31-2022

calibration results. Therefore, ensuring the extraction accuracy of distributed targets and obtaining high-quality reference objects is one of the urgent problems to be solved in the current distributed target polarimetric calibration method.

It is worth noting that the extraction of distributed targets is also widely used in synthetic aperture radar interferometry (InSAR). The extraction process is based mainly on the characteristics of the distributed targets whereby most of the targets belong to surface objects, and the selected homogeneous points are used to determine the distributed targets. Based on the assumption that the neighboring pixels close to the reference pixel are more likely to be homogeneous pixels (Wang et al., 2016), researchers have carried out a series of related studies (Chi et al., 2021). In 2011, Ferretti et al. (2011) applied the Kolmogorov-Smirnov (KS) test to the extraction of homogeneous points.

To solve the problem of low extraction accuracy of distributed objects in images obtained from the polarization feature level by Span et al., this paper proposes a distributed object extraction method combined with hypothesis testing based on the advantages of spatial statistical information. The method utilizes the homogeneous point set obtained by the hypothesis testing method, and adopts the adaptive threshold algorithm to automatically extract the distributed reference samples. In addition, based on the distribution target extraction results, we use the Quegan method to solve the calibration parameters, and finally achieve the calibration of the image. In this paper, the airborne X-band PolSAR is used as the experimental data, and the method in this paper is compared with the traditional extraction methods from the perspectives of qualitative and quantitative. At present, polarimetric calibration is an important prerequisite for polarization information processing, and its innovation and research have important theoretical significance and practical value.

2. MODEL FOR CALIBRATION ERROR

The PolSAR antenna emits electromagnetic waves, irradiates the ground imaging target after being transmitted by the atmosphere, and returns the electromagnetic waves which contain the scattering characteristics of the target to the receiving antenna after undergoing reflection from the target. In this process, due to the influence of channel crosstalk, channel imbalance, and Faraday rotation, the actual measurement and the real scattering matrices of the target do not conform to an equal relationship. Therefore, it is necessary to establish an error model to characterize the relationship between them. The general formula is as follows (Freeman, 1992; Touzi and Shimada, 2009):

$$M = Ae^{j\varphi}RFSFT + N \tag{1}$$

where M is the observed polarization scattering matrix and S is the real polarization scattering matrix in the ideal state. A is the gain factor for the absolute amplitude of the radar system, and φ is the overall phase offset of the system. R and T are parameters of the polarization distortion matrix corresponding to reception and transmission, respectively. F is the Faraday rotation effect caused by the electromagnetic waves passing through the ionosphere, and the transmitting and receiving process will both be affected, therefore, the F rotation matrix needs to be acted on twice; F only affects the polarization determination of spaceborne SAR, especially for L, P, and other long wave SAR data. The airborne SAR data used in the experimental part of this paper are not affected by the Faraday rotation effect, therefore, the Faraday rotation effect in the following formula is ignored. N is the additive noise matrix of the system.

For distributed targets only, the Sinclair matrix cannot be used to give an accurate description. Thus, in the polarimetric calibration method of distributed targets, the polarization covariance matrix C is normally used to describe the distributed targets. Ignoring the noise factor, the covariance matrix C can be obtained by

$$C = \left\langle \overrightarrow{M} \bullet \overrightarrow{M}^{H} \right\rangle \tag{2}$$

where < > represents the spatial average of the matrix, H represents the conjugate transpose. Most of the classical distributed target calibration methods are based on the target's polarization covariance matrix to solve the crosstalk and channel imbalance parameters in turn, and finally complete the data correction for polarization.

3. METHOD

3.1 Calibration methods

Two polarimetric calibration methods are used in this study, one is the Quegan method based on distributed targets, the other is the Whitt method that relies entirely on the solution of the CRs. The Quegan method does not require the CRs to solve the crosstalk and cross-pol channel imbalance, and only needs at least one calibration body to solve the co-pol channel imbalance. Furthermore, the Quegan method does not need iteration, and the expression is easy to implement, thus this method is widely used in airborne PolSAR calibration. Consequently, this study will exploit the proposed distributed target extraction method to further improve the accuracy of the distributed target polarimetric calibration on the basis of this method.

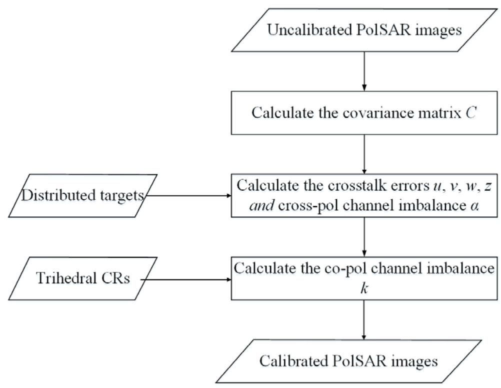

Figure 1. Flow chart of the Quegan method.

The Whitt method, which is based on three different types of artificial CRs, calculates the polarization distortion matrices R and T of transmission and reception, respectively. In practice, a large number of CRs need to be placed on the ground to ensure the accuracy of the method, thus it may not be suitable for application over large areas. However, due to its objectivity and accuracy, the Whitt method can be used as one of the important means to evaluate the accuracy of polarimetric images. Therefore, this method is used to further verify the effectiveness of the improvement in qualitative and quantitative measurement.

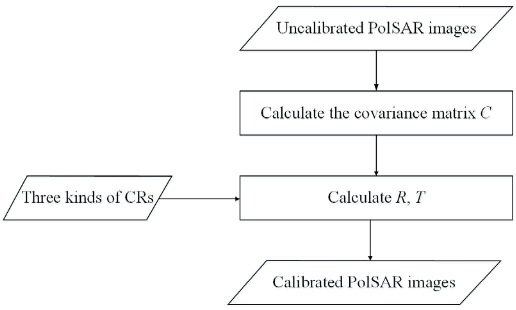

Figure 2. Flow chart of the Whitt method.

3.2 Improved distribution target extraction method

Only using polarization features such as total power Span to extract the results of distributed targets has low accuracy, which will affect the accuracy of subsequent polarimetric calibration methods based on such targets. The homogeneity point selection method, according to the statistical principle, compares the similarity between the central pixel and other pixels in the window, and obtains the number of homogenous points in the window of the central pixel. This method can obtain a large number of homogeneous points in natural distributed features such as farmland and bare soil, but a small number of homogeneous points in urban areas and other areas, and the results of this method can be used to further improve the extraction accuracy of distributed objects in images. Therefore, this paper proposes a distributed target extraction method, which combines polarization features and spatial statistical features, which can not only ensure that saturated pixels and low-power pixels are eliminated at the polarization feature level, and obtain preliminary extraction results. The accuracy of extracting distribution targets is further improved by using spatial statistical information through hypothesis testing methods. The distributed target extraction method proposed in this paper is mainly combined with KS test (A distributed target extraction method Combined with KS, KS-DTEM). The principle is as follows:

The KS test (Ferretti et al., 2011) first calculates the difference in the maximum distance between two probability cumulative distribution functions, and then judges whether the empirical samples are similar. Assuming that the cumulative distribution functions of the intensity information of the reference pixel and its neighboring pixel in the time dimension are $\hat{F}_{ref}(x)$ and $\hat{F}_{neig}(x)$, respectively, the null hypothesis H_0 and the alternative hypothesis H_1 are:

$$H_0 : \hat{F}_{ref}(x)=\hat{F}_{neig}(x) \qquad H_1 : \hat{F}_{ref}(x) \neq \hat{F}_{neig}(x) \tag{3}$$

The statistic $D(x)$ for the maximum distance between the intensity values of the two samples may then be calculated. The expression for calculation is:

$$D(x) = \max_x | \hat{F}_{ref}(x) - \hat{F}_{neig}(x) | \tag{4}$$

After taking the obtained D as the supremum of the KS test, the rejection domain of the different significance levels a can be expressed as follows:

$$D > c_a \sqrt{\frac{2}{N}} \tag{5}$$

where c_a is the a quantile of the KS test distribution, and the number of samples N for the polarization channels of the polarization SAR image is 4. If D is within the rejection domain, the null hypothesis is rejected, and the pixels of the two samples are considered to be significantly different, and the similarity is low; otherwise, H_0 is accepted, and the two samples are considered not to be significantly different, and can be determined as homogeneous points. The KS test is widely used, given that the rejection region of it can be directly calculated without making assumptions about the sample distribution function. However, the low power of the KS test and its insensitivity to the tail of the empirical distribution make the results more prone to failure to reject H_0, leading to a possible increase in Type II errors.

In this paper, the KS test is used to first obtain a set of homogeneous points, and the result is normalized, then OTSU is used to obtain its threshold. Finally retain the homogeneous point pixels larger than the threshold value, and eliminate the heterogeneous point pixels smaller than the threshold value.

4. EXPERIMENT

4.1 Experimental data and corner reflectors

We use a high-resolution airborne PolSAR image to verify the effectiveness of the algorithm. The multi-frequency airborne PolSAR system developed by Chinese Academy of Sciences (IECAS) made its first test flight in 2013. In this part of the experiment, a multi-look X-band image was produced in Zunhua, Hebei, China on September 26, 2013, with an image size of 5461×5461. Figure 3 shows the location of the experimental area and the Pauli RGB image of the scene. The red boxes of G1 and G2 are respectively a group of corner reflectors (CRs) arranged along the distance, including a trihedral angle CR, a 0-degree dihedral angle CR and a 45-degree dihedral angle CR. The specific distribution is shown in the corresponding partial enlarged image. The G1 group is used to obtain the calibration parameters, and the G2 group is used to verify the accuracy in the experiment part.

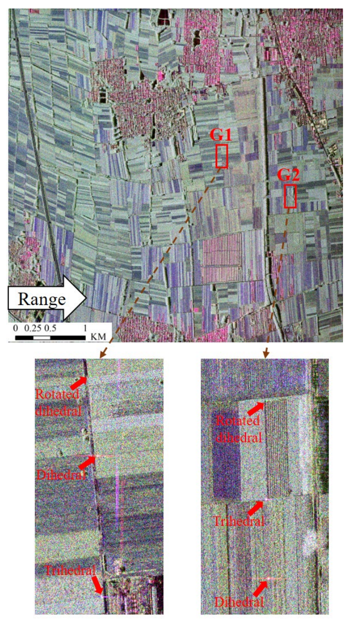

Figure 3. Study area and location of CRs.

4.2 Comparison of distribution target extraction methods

In order to verify the effectiveness of the method proposed in this paper, it is compared with the three commonly used distribution target extraction methods. Figure 4 shows the results of different distribution target extraction methods. The mask result is also a binary image. The white part is 1, indicating the extracted target, which is used for subsequent calibration calculations; while the black part is 0, indicating the pixel that need to be masked out. Figure 4 (a) is the result of using Span (Ainsworth et al., 2006) as the extraction index. This method first calculates the mean $Span_T$ of each column, and then removes the column where the Span is greater than 4 times $Span_T$ and less than 0.02 times $Span_T$. Figure 4 (b) shows the extraction method based on the PCC (Ainsworth et al., 2006; Kimura et al., 2004), which retains the part with the PCC less than 0.5. Figure 4 (c) is a graph of the extraction results based on Helix (Chang et al., 2021), which uses OTSU to automatically calculate the threshold.

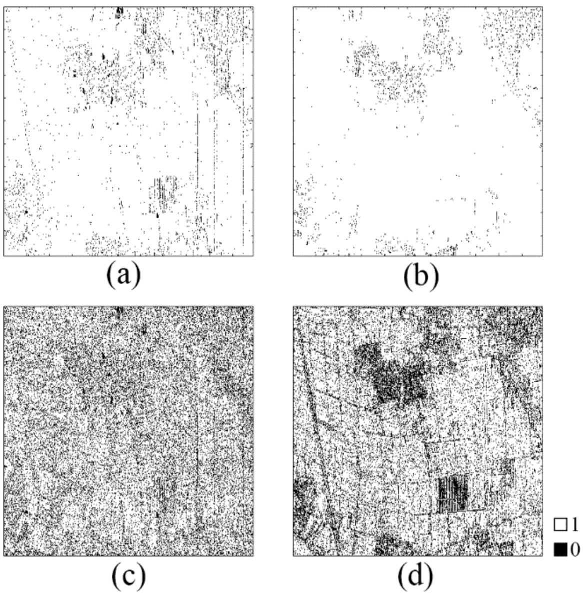

Figure 4. Results of different distribution target extraction methods, (a) Span, (b) PCC, (c) Helix, (d) KS-DTEM.

It can be seen from Figure 4 that the two traditional methods based on polarization characteristics, Span and PCC, can extract large-area distribution target areas such as farmland and bare land. However, many distribution targets were also extracted in residential areas and other areas, and the accuracy of the results was low. Figure 4 (c) shows that the Helix-based extraction method removes more pixels, and extracts relatively more objects only in the bare land, while few objects are extracted in towns, farmland, forests, etc., and the distinguishing effect is not obvious. Figure 4 (d) is the result of the KS-DTEM method proposed in this paper. Compared with other methods, the method in this paper clearly distinguishes different objects. While effectively extracting the distribution target in the image, it can eliminate as many pixels as possible in residential areas and other areas that do not meet the characteristics of the distribution target. The KS-DTEM method combines spatial statistical information to obtain the homogeneous point set through KS, and the OTSU algorithm automatically obtains the distribution target extraction results, which improves the distribution target extraction accuracy and ensures the stability of the subsequent calibration method.

4.3 Polarimetric calibration effect verification

To further verify the effectiveness of the proposed method, the Quegan method is used to calibrate the original PolSAR images based on the distributed target extraction results of different methods. In the process of polarimetric calibration, the trihedral CR in G1 is used to obtain the imbalance of the co-pol channel k, and then the accuracy of the calibrated image is verified by G2. Figure 5 shows the polarization response plots of the trihedral CRs in G1 and G2.

Figure 5 verifies the calibration effect through the polarization response diagram. The calibration based on the four distribution target extraction methods in G1 can correct the distortion of the original uncalibrated image to a certain extent. Their polarization response maps are significantly improved compared to the uncalibrated ones, indicating that these methods can achieve more accurate calibration results. However, there is a trough in the middle of the co-polar corresponding graph in G2, which indicates that there is still a certain unresolved channel imbalance error in the image of the calibration result. This may be because the channel imbalance error varies along the range direction of the SAR image, and the experiment in this paper only uses one trihedral CR in G1 to calibrate the image. There may be some residual error in G2, which is far from the range in which G1 is located.

In order to quantitatively evaluate the accuracy of the calibration results of different methods, this paper uses the Whitt method to calculate the residual errors of the images after calibration based on the Quegan method. At the same time, to further ensure uniformity and objectivity, the CR in G2 is also used in the Whitt method to calculate the crosstalk errors and channel imbalance errors of the calibrated image, where the unit of crosstalk u, v, w, z is dB. Ideally, the crosstalk errors should be negative infinity; the amplitude imbalance of the cross-pol channels α should be as close to 1 as possible, and the corresponding phase imbalance should be as close to 0 as possible.

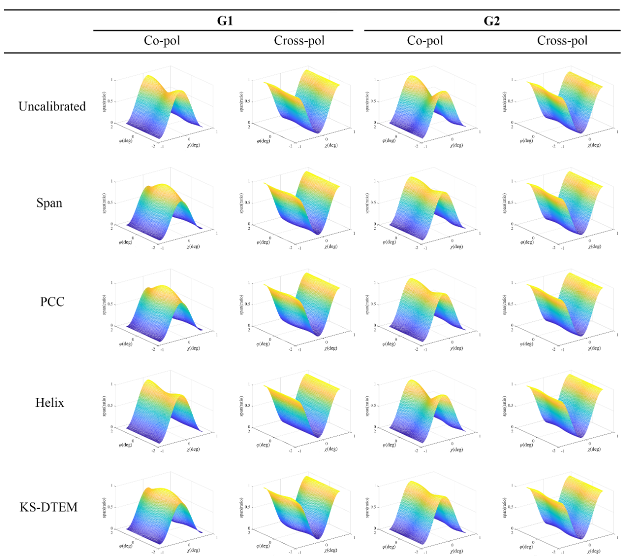

Figure 5. Co-pol and cross-pol response diagrams of trihedral CRs in the two groups of corner reflectors G1 and G2

The quantitative analysis of Table 1 and 2 shows that the errors of uncalibrated images are the largest, indicating the necessity of polarimetric calibration. Span, PCC and Helix methodS can all reduce the crosstalk error in uncalibrated images to a certain extent, and Helix method can obtain the smallest amplitude imbalance of cross-pol channel α, which is 1.20; Span can obtain the smallest phase imbalance of the cross-pol channel α is -0.01. However, these three methods are not optimal in other indicators, and the KS-DTEM method proposed in this paper not only obtains the smallest error in the four crosstalk indicators, which are -38.21 dB, -37.65 dB, -40.38 dB, -35.48 dB; and the result of the cross-pol channel imbalance α is better

	u (dB)	w (dB)	z (dB)	v (dB)
Uncalibrated	-30.25	-29.32	-31.80	-26.80
Span	-32.97	-34.38	-35.39	-31.97
PCC	-33.31	-34.23	-35.69	-31.85
Helix	-32.72	-32.25	-34.33	-30.63
KS-DTEM	-38.21	-37.65	-40.38	-35.48

Table 1. Crosstalk accuracy for different extraction methods

	$\|\alpha\|$	$\angle\alpha$
Uncalibrated	1.52	-0.24
Span	1.32	-0.01
PCC	1.31	-0.03
Helix	1.20	0.03
KS-DTEM	1.28	-0.02

Table 2. Cross-pol channel imbalance accuracy for different extraction methods

and stable. Therefore, in general, different distribution target extraction methods have a certain impact on the accuracy of the calibration results, and compared with other methods, the KS-DTEM method proposed in this paper can not only obtain the clearest extraction results, but also obtain the best calibration result, which improves the accuracy of distributed target extraction and calibration, and proves the effectiveness and advancement of the proposed method in polarimetric calibration.

5. CONCLUSION

In this paper, a KS-DTEM method is proposed to extract distribution targets, which combined with spatial statistical information. The method uses KS to obtain the extraction result of homogenous points, normalizes the result, and compares it with the threshold value automatically calculated by OTSU to determine whether the current pixel is extracted as a distribution target for subsequent calibration calculation. In order to verify the effectiveness of the proposed method, this paper uses X-band PolSAR images in Zunhua, Hebei to conduct experiments. In the experiment, the Quegan method is used to calculate the crosstalk and cross-pol channel imbalance calibration parameters, and then the G1 group of CRs are used to obtain co-pol channel imbalance calibration parameters. In addition, the accuracy of each method is verified from the qualitative and quantitative point of view by using the drawn polarization response images and the residual errors of the G2 group CRs obtained by Whitt method. The experimental results show that compared with the original uncalibrated image, each method can effectively calibrate the PolSAR image, but the proposed method can obtain the optimal value among the four crosstalk indicators, and can obtain stable results in the imbalanced indicators of the co-pol channel. Therefore, in general, the method proposed in this paper has the smallest residual error and the best calibration effect, which further proves that the KS-DTEM method can ensure the accuracy of extracting distributed targets and improve the accuracy of polarimetric calibration. However, the method proposed in this paper still has certain limitations, for example, the calculation of the KS test takes a long time, so the follow-up experiments still need to improve it.

ACKNOWLEDGEMENTS

The authors thank the Chinese Academy of Sciences for their support with the data.

REFERENCES

Ainsworth, T.L., Ferro-Famil, L., Lee, J.-S., 2006. Orientation angle preserving a posteriori polarimetric SAR calibration. IEEE Transactions on Geoscience and Remote Sensing 44, 994-1003.

Chang, Y., Zhao, L., Shi, L., Nie, Y., Hui, Z., Xiong, Q., Li, P., 2021. Polarimetric calibration of SAR images using reflection symmetric targets with low helix scattering. International Journal of Applied Earth Observation and Geoinformation 104.

Chi, B., Fan, H., Gao, Y., Zhao, L., Zhuang, H., 2021. A distributed scatterers InSAR method based on adaptive window with statistically homogeneous pixel selection for mining subsidence monitoring. Geocarto International, 1-24.

Ferretti, A., Fumagalli, A., Novali, F., Prati, C., Rocca, F., Rucci, A., 2011. A New Algorithm for Processing Interferometric Data-Stacks: SqueeSAR. IEEE Transactions on Geoscience and Remote Sensing 49, 3460-3470.

Freeman, A., 1992. SAR calibration: an overview. IEEE Transactions on Geoscience & Remote Sensing 30, 1107-1121.

Imani, M., 2021. A random patches based edge preserving network for land cover classification using Polarimetric Synthetic Aperture Radar images. International Journal of Remote Sensing 42, 4942-4960.

Jäger, M., Scheiber, R., Reigber, A., 2019. Robust, Model-Based External Calibration of Multi-Channel Airborne SAR Sensors Using Range Compressed Raw Data. Remote Sensing 11.

Kimura, H., Mizuno, T., Papathanassiou, K.P., Hajnsek, I., 2004. Improvement of polarimetric SAR calibration based on the Quegan algorithm, IEEE International Geoscience & Remote Sensing Symposium.

Klein, J.D., 1992. Calibration of complex polarimetric SAR imagery using backscatter correlations. IEEE Transactions on Aerospace & Electronic Systems 28, 183-194.

Lee, J.S., Pottier, E., 2009. Polarimetric Radar Imaging : From basics to applications. Polarimetric Radar Imaging : From basics to applications.

Mandal, D., Kumar, V., McNairn, H., Bhattacharya, A., Rao, Y.S., 2019. Joint estimation of Plant Area Index (PAI) and wet biomass in wheat and soybean from C-band polarimetric SAR data. International Journal of Applied Earth Observation and Geoinformation 79, 24-34.

Niu, C., Zhang, H., Liu, W., Li, R., Hu, T., 2021. Using a fully polarimetric SAR to detect landslide in complex surroundings: Case study of 2015 Shenzhen landslide. ISPRS Journal of Photogrammetry and Remote Sensing 174, 56-67.

Park, S.E., Lee, S.G., 2019. On the Use of Single-, Dual-, and Quad-Polarimetric SAR Observation for Landslide Detection. ISPRS International Journal of Geo-Information 8.

Quegan, S., 1994. A unified algorithm for phase and cross-talk calibration of polarimetric data-theory and observations. IEEE Transactions on Geoscience and Remote Sensing 32, 89-99.

Sajjad, E.Z., Yasser, M., Seyed Ali, S., 2019. Assessing the performance of indicators resulting from three-component Freeman–Durden polarimetric SAR interferometry decomposition at P-and L-band in estimating tropical forest aboveground biomass. International Journal of Remote Sensing 41, 433-454.

Sinclair, G., 1950. The Transmission and Reception of Elliptically Polarized Waves. Proc Ire 38, 148-151.

Touzi, R., Hawkins, R.K., Cote, S., 2013. High-Precision Assessment and Calibration of Polarimetric RADARSAT-2 SAR Using Transponder Measurements. IEEE Transactions on Geoscience & Remote Sensing 51, 487-503.

Touzi, R., Shimada, M., 2009. Polarimetric PALSAR Calibration. IEEE Transactions on Geoscience & Remote Sensing 47, 3951-3959.

Van Zyl, J.J., 1990. Calibration of polarimetric radar images using only image parameters and trihedral corner reflector responses. IEEE Transactions on Geoscience & Remote Sensing 28, 337-348.

Wang, Y., Deng, Y., Fei, W., Wang, R., Song, H., Wang, J., Li, N., 2016. Modified Statistically Homogeneous Pixels' Selection With Multitemporal SAR Images. IEEE Geoscience and Remote Sensing Letters 13, 1930-1934.

Whitt, M.W., Ulaby, F.T., Polatin, P., Liepa, V.V., 1991. A general polarimetric radar calibration technique. IEEE Transactions on Antennas and Propagation 39.

Zebker, H.A., van Zyl, J.J., Held, D.N., 1987. Imaging radar polarimetry from wave synthesis. Journal of Geophysical Research 92.